

# Effect of Atmospheric Transmission and Radiance on Aircraft Infrared Signatures

G. A. Rao\* and S. P. Mahulikar†

Indian Institute of Technology—Bombay, Powai, Mumbai 400 076, India

This paper elaborates the role of atmosphere in determining infrared signatures of aircraft as perceived by a ground-based infrared detector, similar to the case of an infrared guided heat-seeking surface-to-air missile. The main objectives are to assess the effect of atmosphere on aircraft infrared signature and to evaluate infrared bands in which a conventional fighter-class aircraft is most susceptible to infrared guided missiles. Such an analysis is of paramount importance for aircraft infrared signature management and aircraft mission planning. First, the lock-on range is derived as a function of aircraft, missile seeker, and atmospheric parameters. Thus, the role of atmospheric radiance and transmittance in determining aircraft signature level as perceived by the missile infrared seeker is brought out. The role of various atmospheric constituents in dictating infrared characteristics of the atmosphere is also discussed. The Berger's model is used for computing atmospheric/sky radiance and the Lowtran-7 model to compute atmospheric transmissivity. The infrared bands in which the aircraft signature is prominent are identified, and the variation of aircraft signature level and lock-on range with respect to a typical surface-to-air missile within these bands are analyzed and discussed for a representative case.

## Nomenclature

$A$	=	area, $\text{m}^2$
$E$	=	emissive power, $\text{W} \cdot \text{m}^2$
$J$	=	radiance, $\text{W} \cdot \text{m}^{-2} \cdot \text{Sr}^{-1}$
$J_\lambda$	=	spectral radiance, $\text{W} \cdot \text{m}^{-2} \cdot \text{Sr}^{-1} \cdot \mu\text{m}^{-1}$
$N$	=	irradiance, $\text{W} \cdot \text{m}^{-2}$
$R$	=	range, $\text{m}$
$S$	=	signal, $\text{W} \cdot \text{m}^{-2}$
$T$	=	temperature, $\text{K}$
$\varepsilon$	=	emissivity, —
$\lambda$	=	wavelength, $\mu\text{m}$
$\sigma$	=	Stefan–Boltzmann constant = $5.67 \times 10^{-8} \text{ W} \cdot \text{m}^{-2} \cdot \text{K}^{-4}$
$\tau$	=	atmospheric transmissivity, —
$\omega$	=	solid angle, $\text{Sr}$

## Subscripts

$ac$	=	aircraft
$b$	=	background
$dp$	=	dew point
$g$	=	ground

## Introduction

**F**IGHTER aircraft should exhibit a high degree of survivability in a hostile environment to complete their assigned missions. To increase their survivability, aircraft attempt to evade detection from enemy antiaircraft defense systems by reducing their observables. Infrared radiation (IR) emitted by aircraft is a passive means of detection for enemy IR-guided heat-seeking missiles, which are proven to be more lethal than active means of aircraft detection and tracking.<sup>1</sup> In the past few decades, IR-guided fire-and-forget

missiles have emerged as a major threat to military aircraft, especially in the wake of increased usage of such missiles by terrorist groups.

Because atmosphere surrounds the aircraft and the IR-guided missile, IR characteristics of the atmosphere have a significant role in dictating the aircraft signature as perceived by the missile. Often, studies involving IR signature modeling reported in literature make simplistic assumptions regarding atmospheric IR characteristics. Such assumptions can alter the computed aircraft IR signature by a nonnegligible amount, which in turn can alter aircraft susceptibility analysis. Also, the choice of the detector's operating wavelength band used on IR-guided missiles depends on the environment in which the missile is expected to perform. It is thus important to study atmospheric IR characteristics and their effect on aircraft IR signatures.

An integrated overview of aircraft stealth technology and the importance of infrared signatures is elaborated by Rao and Mahulikar.<sup>1</sup> Accurate IR signature modeling can be used to substantially reduce aircraft susceptibility to IR-guided threats. An overview of modeling techniques for evaluating aircraft IR signatures produced by sources such as engine casing, exhaust plume, and airframe is discussed by Mahulikar et al.<sup>2</sup>

## Motivation

Infrared-guided heat-seeking missiles have been responsible for downing more than 89% of aircraft and helicopters from 1979 to 1993.<sup>3</sup> Also, the advances in IR detectors have increased detection capabilities of missiles by several times.<sup>4,5</sup> Some of the common heat-seeking IR-guided missiles and their origin are listed by Rao and Mahulikar.<sup>1</sup> Aircraft IR signature modeling is an important part of stealth technology, and is used for the following:

- 1) Susceptibility assessment of aircraft against IR-guided threats.
- 2) Designing advanced IR signature suppression systems for helicopters<sup>6,7</sup> and aircraft.
- 3) Aircraft mission planning in a tactical warfare for susceptibility reduction. For instance, threats from IR-guided surface-to-air missiles (SAMs) can be reduced by planning the flight envelope such that aircraft IR footprint on the ground is minimized.

## Objective and Scope

The objective of this investigation is to assess the effect of atmospheric transmittance and radiance (sky radiance) on aircraft IR signatures, and to identify IR bands in which a typical fighter aircraft is most susceptible to IR-guided SAMs. The atmospheric IR

Received 11 January 2004; revision received 9 June 2004; accepted for publication 10 June 2004. Copyright © 2004 by the American Institute of Aeronautics and Astronautics, Inc. All rights reserved. Copies of this paper may be made for personal or internal use, on condition that the copier pay the \$10.00 per-copy fee to the Copyright Clearance Center, Inc., 222 Rosewood Drive, Danvers, MA 01923; include the code 0021-8669/05 \$10.00 in correspondence with the CCC.

\*Research Scholar, P.O. IIT, Department of Aerospace Engineering. Student Member AIAA.

†Faculty Member and A. von Humboldt Fellow, P.O. IIT, Department of Aerospace Engineering; spm@aero.iitb.ac.in.

characteristics studied here are confined to a few representative atmospheric conditions and specified IR spectra of interest to tactical military operations.

### Aircraft Lock-on Range

The IR signature of an aircraft as perceived by a missile is the contrast in IR emission between the aircraft surface (as transmitted by atmosphere) and the background radiance within the detector's operating wavelength band (in which the detector has good responsivity). The maximum detection range of an IR detector depends on its noise equivalent irradiance (NEI),<sup>8</sup> performance feature of the detector system, and the contrast between target aircraft and background radiance. The total radiation incident on the IR detector is the sum of target radiance as transmitted by the intervening atmosphere and background sky radiance (which is due to the emission by radiation-participating gases in the atmosphere), as illustrated in Fig. 1. Assuming that the detector's field of view is not completely filled by target aircraft (the solid angle subtended by the aircraft at the detector is less than the detector's field of view), irradiance on the detector is given as

$$N = J_{ac} \cdot \omega_{ac} \cdot \tau + J_b \cdot (\omega_d - \omega_{ac}) \quad (1)$$

where  $\omega_{ac}$  is the solid angle subtended by aircraft at the detector, given by  $A_{ac}/R^2$ , and  $\omega_d$  is the detector's field of view.

Most IR detection systems use reticles to modulate the incident radiation. This modulation is used to track the target in azimuth and to discriminate the target against its background, thereby improving the detector signal-to-noise ratio. Hence, the radiant signal incident on the detector can be obtained as

$$N = (J_{ac} \cdot \tau - J_b) \cdot (A_{ac}/R^2) \quad (2)$$

where  $A_{ac}$  is the normal projected area of the aircraft. The detection range is now obtained as

$$R^2 = (J_{ac} \cdot \tau - J_b) A_{ac} / N \quad (2.1)$$

The maximum detection range (when signal is equal to noise) is obtained by replacing  $N$  with NEI as

$$R_{max} = [(J_{ac} \cdot \tau - J_b) A_{ac} / \text{NEI}]^{0.5} \quad (3)$$

Thus, the maximum detection range is directly proportional to the square root of target contrast radiance and the target's projected normal area. After the target aircraft is detected, the missile IR seeker locks-on to the target aircraft; that is, the missile automatically tracks its target. The maximum range at which this occurs is the lock-on

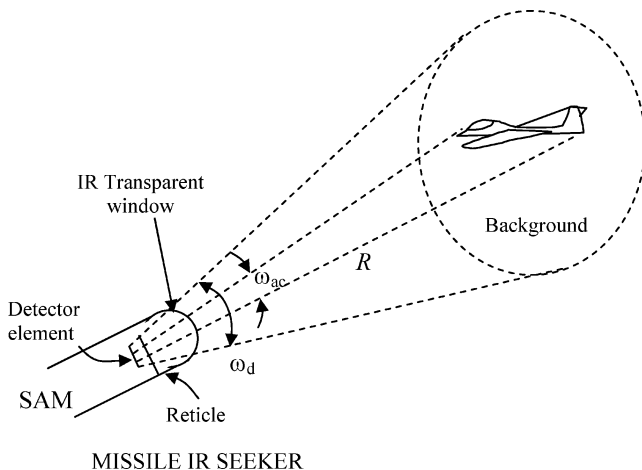


Fig. 1 Schematic of seeker head of IR-seeking missile and its instantaneous field of view.

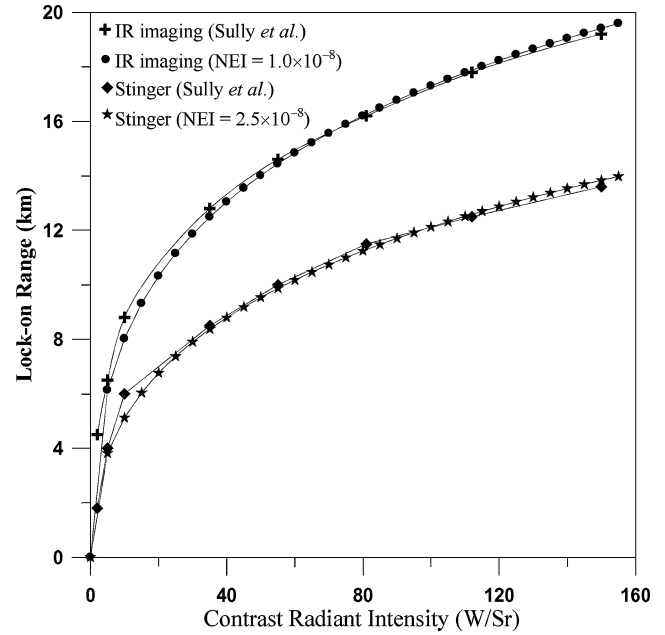


Fig. 2 Aircraft IRSL versus lock-on range plots for various IR detectors in the mid-IRSL (NEI, W/m<sup>2</sup>).

range (the signal from the target aircraft should also cross some minimum threshold value for initiation of tracking, determined by  $\xi_{min}$ ). Hence, the maximum range where lock-on occurs is calculated as

$$R_{LO} = [(J_{ac} \cdot \tau - J_b) A_{ac} / (\text{NEI} \cdot \xi_{min})]^{0.5} \quad (4)$$

Thus, the atmosphere has two important roles in evaluation of aircraft IR signatures. First, the transmissivity of the atmosphere dictates which part of IR radiation emitted by the aircraft reaches the missile and in what amount. Second, the atmospheric radiance forms the background infrared radiation against which the missile IR detector distinguishes aircraft IR emission. Both these phenomena reduce the total amount of IR signature as perceived by the detector, and hence are beneficial from an aircraft survivability point of view. Therefore, it is important that the IR radiation characteristics of atmosphere are modeled correctly and accurately.

From Eq. (4), lock-on range is plotted against aircraft infrared signature level (IRSL) in the band 3.2–4.2  $\mu\text{m}$  (shown in Fig. 2). The computed values are compared with the plots given by Sully et al.<sup>3</sup> for IR imaging and Stinger missile. The computed values are in good agreement with those obtained by Sully et al. The imaging IR detector has a lower NEI as compared to the IR detector on the Stinger, and therefore the imaging IR detector has a higher lock-on range for the same aircraft IRSL.

### Atmospheric Infrared Characteristics

Even though nitrogen and oxygen are the major constituents of the atmosphere, the radiative characteristics of the atmosphere are primarily governed by carbon dioxide ( $\text{CO}_2$ ), water vapor ( $\text{H}_2\text{O}$ ), and ozone ( $\text{O}_3$ ). These three gases are responsible for maintaining the atmospheric temperature within limits conducive to life. There are other trace gases with asymmetrical molecular structures affecting atmospheric IR characteristics, such as  $\text{CH}_4$  and oxides of nitrogen, but their contribution is small. The concentration of ozone is prominent only at an altitude of 20–30 km. The concentration of water vapor decreases rapidly with altitude and is absent above 10 km. The pressure, temperature, and concentration of the participating gases influence infrared transmission and emission. Radiative characteristics of the atmosphere are a function of many parameters: temperature, humidity, weather conditions, composition, and so

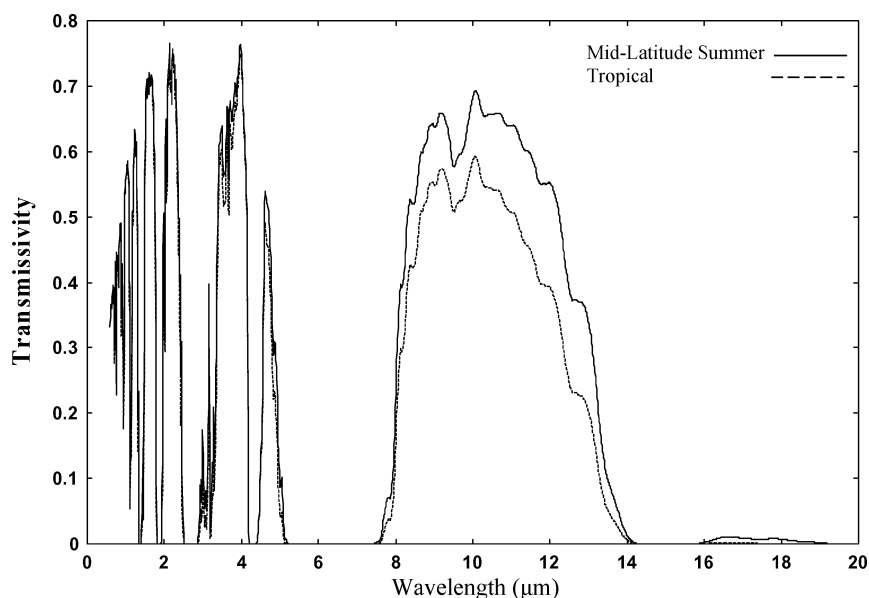


Fig. 3 Atmospheric transmissivity for midlatitude summer and tropical conditions.

forth. Therefore, considering different atmospheric conditions leads to different computed predictions of aircraft IRSIs. For purposes of comparison and uniformity, here the target aircraft is considered in a clear cloudless night sky to calculate the contrast produced on a ground-based SAM.

#### Atmospheric Transmissivity

The atmosphere is a good absorber of IR radiation. Radiant flux from the aircraft is selectively absorbed by several atmospheric gases and scattered away by suspended particles in atmosphere (e.g., aerosols). There are a few bands in the total IR spectrum where atmospheric absorption is low and transmissivity of IR radiation is high; these wavelength bands are commonly known as atmospheric windows. For purposes of aircraft detection and tracking as used in antiaircraft missiles, the IR detector must operate within these atmospheric windows.

Several databases are available for evaluating atmospheric transmissivity under various atmospheric conditions. One such model is LOWTRAN. It is a low-resolution atmospheric transmissivity model, which can be used for wavelengths longer than  $0.2 \mu\text{m}$  at a spectral resolution of  $20 \text{ cm}^{-1}$  (Refs. 9, 10). LOWTRAN is based on band models of molecular absorption and was first released in 1972. The LOWTRAN-7 code is used in the present analysis for computing atmospheric transmissivity. Figure 3 shows atmospheric transmissivity obtained using the LOWTRAN model for a vertical path length of 5 km for midlatitude summer and tropical conditions between 1 and  $20 \mu\text{m}$  (when an aircraft is flying directly over the detector, i.e., at zenith). As seen from Fig. 3, there exist many atmospheric windows, some of which are too narrow and insignificant. The atmospheric window between 8 and  $14 \mu\text{m}$  is the widest. Also, atmospheric transmissivity after  $14 \mu\text{m}$  is negligible, and hence these wavelengths can not be harnessed for aircraft detection. The transmissivity is higher for midlatitude summer conditions, especially in the band 8– $14 \mu\text{m}$ .

#### Atmospheric Radiance

As discussed earlier, atmospheric radiance is the background radiation noise for IR detectors and is responsible for reducing the total aircraft IR signature level. The spectral distribution of atmospheric radiation is mainly due to thermal emission by atmospheric gases and by the scattering of sunlight. However, scattering of radiation by particles in atmosphere is prominent only in the visible and near infrared bands of the electromagnetic spectrum. Studies have shown that a very small quantity of light is scattered at wavelengths

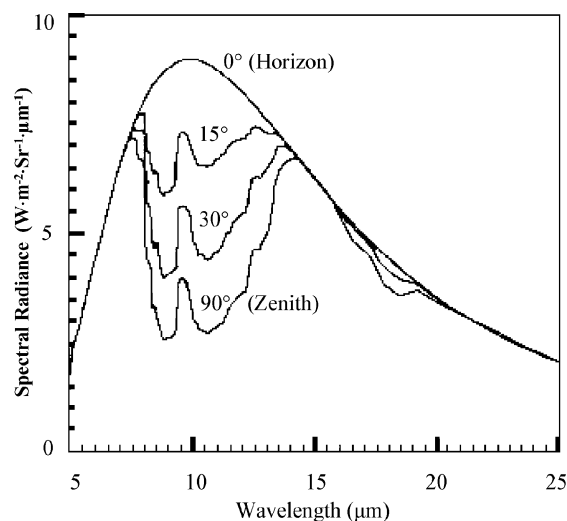


Fig. 4 Spectral clear sky radiance on ground for midlatitude summer.

above  $2 \mu\text{m}$ , and a negligible quantity beyond  $4 \mu\text{m}$  (Ref. 11). Also, scattering is observed only during the daytime.<sup>12</sup> Hence, scattering can be safely neglected for evaluation of atmospheric radiance in this investigation.

The spectral radiance of the sky as received by an IR detector on the ground for midlatitude summer ( $T_g = 21^\circ\text{C}$  and  $T_{dp} = 16^\circ\text{C}$ ) atmospheric conditions<sup>13</sup> is shown in Fig. 4. It is seen that as the view angle approaches the horizon (0 deg) from the zenith (90 deg), the spectral radiance of the atmosphere becomes similar to that of a blackbody at ground level temperature. This is due to the increase in optical path length of the atmosphere. At ground level, the atmospheric radiance is dominated by  $\text{H}_2\text{O}$  (vapor.), whose concentration may vary from 0.2 to 4% by volume, depending on the temperature and humidity. The peak observed around  $9.6 \mu\text{m}$  is due to emission by ozone. Radiation by  $\text{CO}_2$  is prominent around  $4.3 \mu\text{m}$  because of its vibrational band, but at this wavelength, the spectral emissive power of the atmosphere is negligible and hence is not of any significance.

Some investigators, while evaluating IR signatures of aircraft, have approximated the background sky radiation as that of a blackbody at ground-level temperature or at aircraft ambient temperature.<sup>2,14</sup> The wavelength of maximum IR emission for

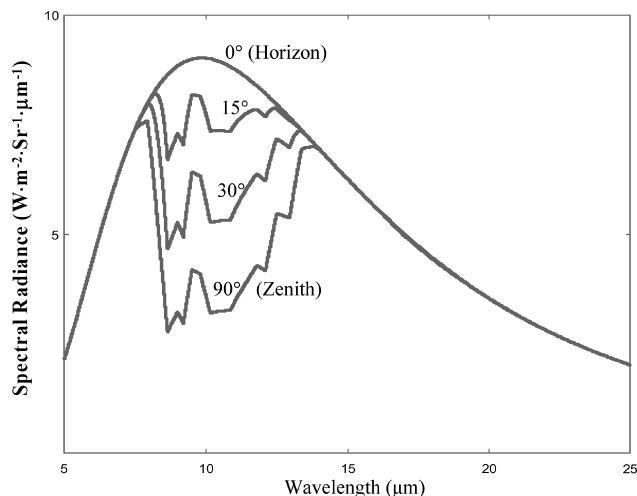


Fig. 5 Spectral clear sky radiance for midlatitude summer from Berger's model.

atmospheric radiation lies around  $9.5 \mu\text{m}$ . The effect of background radiation on the aircraft IR signature in the band  $8\text{--}12 \mu\text{m}$  is pronounced because background radiation is dominant in this band, but is negligible in the near and mid IR bands.

Several studies have been carried out to determine clear sky emissivity. Some investigators have determined the total equivalent emissivity of clear skies for various conditions from the statistical analysis of experimental data gathered over a period at many places and in a variety of weather conditions.<sup>13,15,16</sup> Berger<sup>17</sup> developed a simple model for evaluation of spectral emissivity, and hence spectral radiance of the atmosphere, as a function of ground-level temperature and dew point temperature (a function of relative humidity). This model can also be used to determine the total and the directional spectral emissivity of clear sky.<sup>18,19</sup> The model approximates sky radiance to that of a blackbody at ground-level temperature below  $7.5 \mu\text{m}$ , between  $14.00$  and  $16.25 \mu\text{m}$ , and beyond  $22.5 \mu\text{m}$ . Mainly, the effect of water vapor absorption and ozone (at  $9.6 \mu\text{m}$ ) is taken into account. The radiance at  $4.3 \mu\text{m}$  due to  $\text{CO}_2$  is neglected because atmospheric radiance below  $5 \mu\text{m}$  is negligible. The total spectrum is divided into a number of parts and absorption coefficients are tabulated from the least-squares fit for data obtained over a period of time for various atmospheric conditions. In addition, the model can evaluate differences in sky radiance between day and night. Figure 5 shows spectral radiance of the sky obtained by Berger's model for the conditions in Fig. 4.

The LOWTRAN-7 model used for computing atmospheric transmissivity can also be used for computing atmospheric radiance, but the Berger's model has been used here because of the following reasons:

- 1) The Berger model is simpler and easier to implement than the LOWTRAN-7 model.
- 2) The values obtained by the Berger model compare well with experimental values.
- 3) Berger's model is computationally faster than LOWTRAN-7. Because the entire analysis is carried out for spectral quantities, use of Berger's model has reduced the computational time substantially.

The main limitations of Berger's model are as follows:

- 1) It can be seen from the comparison of Figs. 5 and 6 that Berger's model predicts sky radiance accurately, except at  $16\text{--}20 \mu\text{m}$ . Nevertheless, this is not significant, as it lies outside the atmospheric windows of interest and is inconsequential for aircraft IR signature analysis.
- 2) Because radiation predicted by Berger's model is a function of  $T_g$  and  $T_{dp}$ , the model can be used only to predict atmospheric radiation on the ground, and not at higher altitudes. Hence, Berger's model cannot be used in the case of air-to-air missiles (AAMs) that are air-launched from aircraft.

Figure 6 shows the background sky radiance for various assumptions, namely, radiance when the background is considered as a

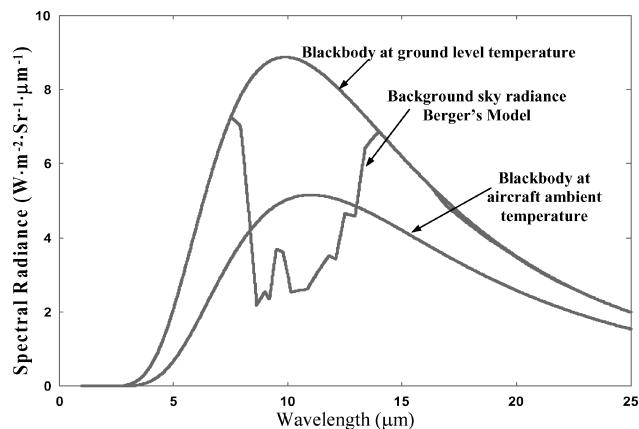


Fig. 6 Background sky radiation for various assumptions.

blackbody at ground level temperature, radiance as calculated by using Berger's model, and background radiance considered as a blackbody at aircraft ambient temperature (altitude of  $5 \text{ km}$ ). It is seen that sky radiance evaluated by Berger's model is less than that obtained by assuming sky radiation as a blackbody in the band  $8\text{--}12 \mu\text{m}$ . It is clear from Fig. 6 that assuming the background to be a blackbody would compute low values of IR signature in the atmospheric window at  $8\text{--}12 \mu\text{m}$  (also called the second atmospheric window).

### Aircraft Infrared Signature

The main sources of IR signature in aircraft are power plant, exhaust plume, and airframe.<sup>1,2</sup> Among these sources, power plant is the major source of IR emission because of the large amount of heat produced by combustion inside the gas turbine engine. The exhaust plume is at high temperature and emits IR radiation because of radiating gases such as  $\text{H}_2\text{O}$  (vapor),  $\text{CO}_2$ , and  $\text{CO}$  present in the plume. During high-speed flight, aerodynamic heating of the airframe is significant and can contribute substantially to the overall aircraft IR signature.

The roles of contributors to aircraft IR signature change with aircraft aspect. From the frontal aspect, the airframe is the main contributor. The leading edges of wings and the stagnation region of the aircraft nose are heated aerodynamically at high Mach numbers. The IR signature from the airframe is not prominent from other aspects and at low flight speeds. From the side aspect, the aircraft rear fuselage heated by the embedded engine and the exhaust plume are major contributors. From the rear aspect, signature from the hot engine tailpipe is prominent.

The aircraft rear fuselage and engine tailpipe behave like gray bodies and emit radiation in the entire IR spectrum, unlike the exhaust plume, which emits only in selected narrow wavelength bands depending on the temperature, pressure, and composition of radiating gases in the plume. In the nonafterburning mode (dry mode), the plume radiation is substantially less than that from the engine tailpipe and the exposed rear fuselage. Since the aircraft is in dry mode for most of the time, in the present analysis, the IR signature produced by the rear fuselage and engine tailpipe is considered. Other sources such as exhaust plume and leading edges of wings are neglected. The spectral radiance of a typical single-engine fighter aircraft rear fuselage and engine tailpipe, flying at a speed of Mach 0.8 and at an altitude of  $5 \text{ km}$  in the dry mode, is shown in Fig. 7. Though the spectral radiance of the rear fuselage is less than that of the tailpipe, the IR emission from the rear fuselage is important because

- 1) The projected area of the fuselage is greater than that of the tailpipe; hence, the projected solid angle on the IR detector is greater.
- 2) When the aircraft is approaching the missile site, the tailpipe is not visible to the ground-based IR seeker, and the rear fuselage becomes the major contributor of aircraft IR signature. This is especially important during the ingress (dash-in) mode of the mission leg

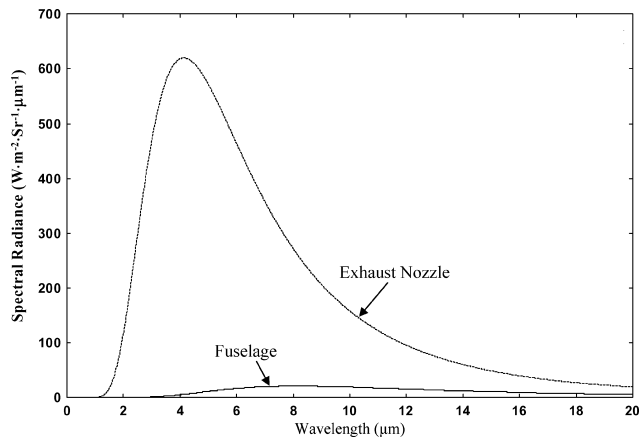


Fig. 7 Spectral radiance of aircraft rear fuselage.

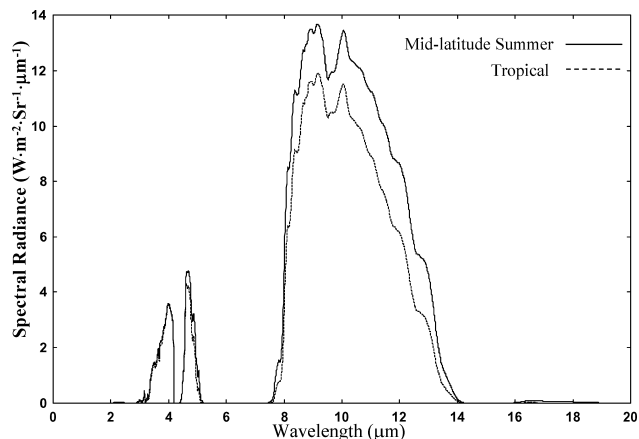


Fig. 8 Aircraft rear fuselage radiance as transmitted by the intervening atmosphere.

when the aircraft is more susceptible to antiaircraft missiles because of higher relative velocity between aircraft and missile.

3) The rear fuselage is visible from wider view angles than the engine tailpipe.

Modeling the spectral intensity of the engine tailpipe is simple; the tailpipe forms a cavity and can be approximated like a gray body with high emissivity ( $\approx 0.9$ ) at exhaust gas temperature.<sup>8</sup> For modeling emission from the aircraft rear fuselage, the temperature distribution over the fuselage has to be determined for the given engine operating conditions. This is difficult because all the modes of heat transfer are involved simultaneously, resulting in integrodifferential governing equations that are difficult to solve. A detailed model to compute rear fuselage temperature distribution for given engine operating conditions is given by Mahulikar et al.<sup>20</sup> The rear fuselage temperature is obtained from steady state multimode heat transfer modeling of the engine layout, which includes surface radiation interchange in conjunction with internal and external convection.

In this investigation, the spectral reflection of radiation from the ground terrain<sup>21</sup> off the fuselage is also considered. The spectral radiance of the aircraft rear fuselage (Fig. 7) as transmitted by the mid-latitude summer atmosphere and tropical atmosphere (see Fig. 3) is shown in Fig. 8. It is seen that the intervening atmosphere does not transmit IR radiation from the aircraft to the ground-based IR detector outside the atmospheric windows. Hence, the IR detector cannot detect aircraft outside the atmospheric windows.

Figure 9 shows the contrast between aircraft IR emission and background radiance (predicted using Berger's model in Fig. 5) received by an IR detector on the ground for tropical and midlatitude summer atmospheric conditions. The negative radiance in some wavelength bands is because atmospheric radiance in these wavelength bands is greater than aircraft radiance. The highest radiance

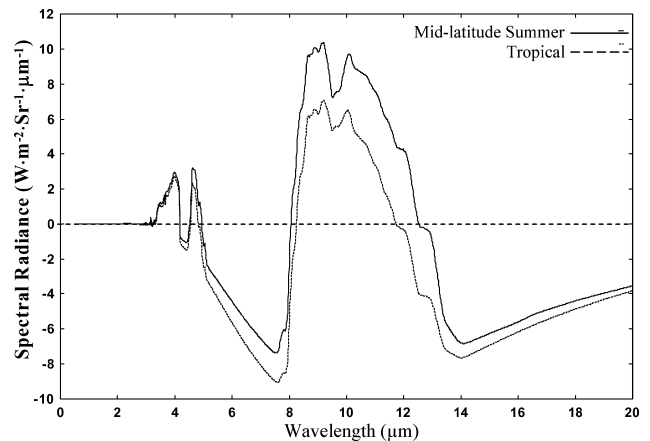


Fig. 9 Spectral radiance contrast as received by the ground-based IR seeker.

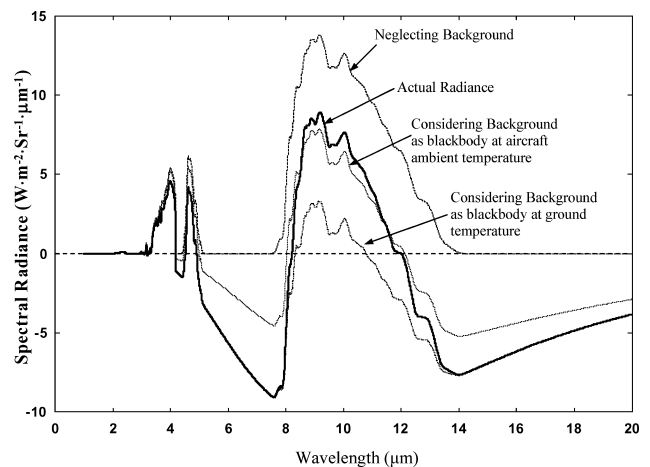


Fig. 10 Aircraft IR signature computed for various assumptions of atmospheric radiance.

is received in the window at 8–12  $\mu\text{m}$ . The aircraft signature received by the ground-based IR detector is prominent only in three wavelength bands as shown in the figure. The band at 8–12  $\mu\text{m}$  is the most prominent for aircraft rear fuselage.

Figure 10 shows the effect of background sky/atmospheric radiance on the computed IR signature of aircraft rear fuselage in the nonafterburning mode. It is observed that when the sky radiance is neglected, the IR signature evaluated is more than 25% higher in the atmospheric band at 8–12  $\mu\text{m}$ . The other two bands (3.24–4.18  $\mu\text{m}$  and 4.50–4.93  $\mu\text{m}$ ) are not much affected because atmospheric radiance is negligible in these bands. Assuming the background sky radiance to be that of a black body at ground-level temperature (shown in Fig. 6) underestimates aircraft signature by more than 50% in the band 8–12  $\mu\text{m}$ . When the aircraft IR signature is evaluated by assuming background radiance to be that of a blackbody at the aircraft ambient temperature at altitude of 5 km, the estimated aircraft IR signature is in close agreement with that evaluated using Berger's model (error less than 5%).

The procedure for evaluating aircraft IRSL (from rear fuselage and engine tailpipe) and lock-on range for an aircraft against a given missile is in Fig. 11. The Berger's model and LOWTRAN-7 code described in the previous section are used to model atmospheric infrared characteristics.

## Results and Discussion

To compute typical fighter aircraft IR signatures and analyze the effect of atmospheric variables on them, a simplistic representative case is considered, where in a fighter aircraft cruising at a constant altitude of 5 km approaches a ground-based missile site and

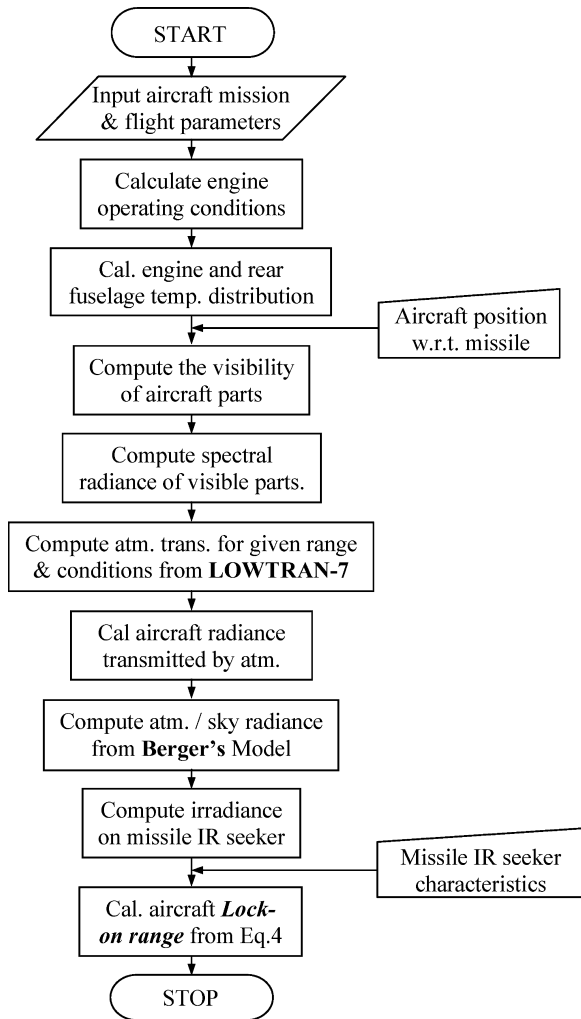


Fig. 11 Procedure for evaluating aircraft infrared signature level and lock-on range.

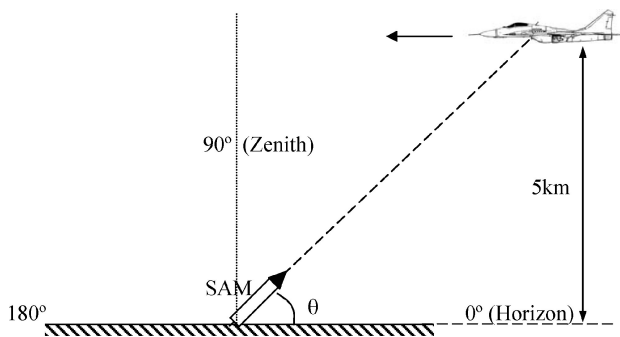


Fig. 12 Aircraft flying over a SAM site.

then passes over it, as shown in Fig. 12. Figure 13 shows the irradiance (signal) on the IR detector of a typical SAM produced by aircraft rear fuselage when the aircraft is directly above the missile (zenith), for midlatitude summer and tropical atmosphere. In this case, the engine tailpipe is not visible to the IR seeker and hence only infrared emission by the rear fuselage is taken into account. The IR signature is prominent in the bands, 3.24–4.18, 4.50–4.93, and 8.20–11.80  $\mu\text{m}$ .

Figure 14 shows the signal obtained for a similar case when the aircraft is at an angle of 120 deg from the horizon. In this case, aircraft IR signature is contributed by both engine tailpipe and rear fuselage. Irradiance on the missile IR seeker is significant in five wavelength bands, 1.95–2.50, 2.92–3.20, 3.24–4.18, 4.50–4.93, and

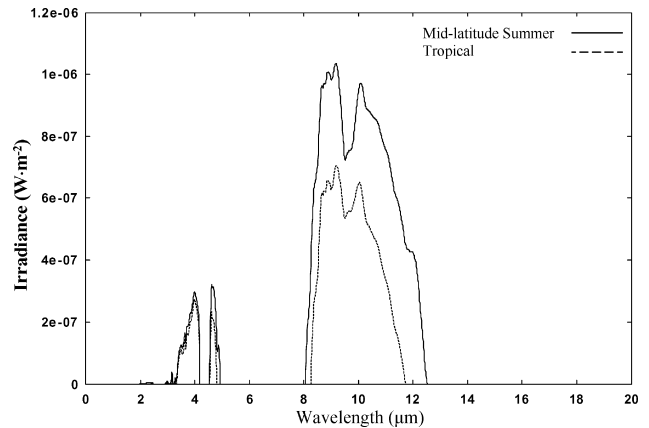


Fig. 13 Irradiance on missile IR detector: aircraft at zenith.

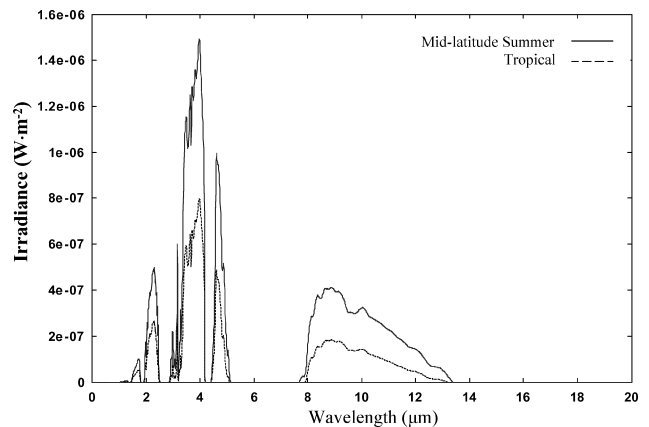


Fig. 14 Irradiance on missile IR detector: aircraft at 120 deg from horizon.

8.2–11.8  $\mu\text{m}$ . The bands at 1.95–2.50 and 2.92–3.20  $\mu\text{m}$  are due to tailpipe emission only.

For the case shown in Fig. 12, where a fighter aircraft cruising at an altitude of 5 km passes over a ground-based missile site, the average signal produced by the missile IR seeker in each of the five bands (1.95–2.5, 2.92–3.20, 3.24–4.18, 4.50–4.93, and 8.2–11.8  $\mu\text{m}$ ) for tropical and midlatitude summer atmospheric conditions is shown in Figs. 15–19. The minimum signal required by the missile IR seeker to lock onto the aircraft is assumed to be 0.25  $\mu\text{W}/\text{m}^2$ . Whenever aircraft signature level increases beyond this threshold level, the missile is capable of locking onto the aircraft. The aircraft signature level is greater in the rear aspect due to visibility of hot engine tailpipe. This level is highest in the band 3.24–4.18  $\mu\text{m}$ . The aircraft rear fuselage contributes primarily to the aircraft IR SL in the forward aspect in the band 8–12  $\mu\text{m}$ , in other bands the contribution is insignificant. Also, the aircraft signature levels for midlatitude summer conditions are higher than those for tropical atmosphere. This is due to the combined effect of high atmospheric transmissivity and lower background radiance for midlatitude summer conditions.

Figures 20–24 show the variation in aircraft lock-on range in each of the five bands (1.95–2.50, 2.95–3.20, 3.24–4.18, 4.50–4.93, and 8.20–11.80  $\mu\text{m}$ ) for tropical and midlatitude summer conditions for the same case as shown in Figs. 15–18. The lock-on range has been calculated against a typical SAM. The lock-on range is greater in the aircraft rear aspect due to high IR signature levels contributed by the engine tailpipe. Since the signature level is higher in the mid-IR band of 3.24–4.18  $\mu\text{m}$ , the lock-on range is also maximum in this band, and exceeds well beyond the distance between the missile and the aircraft. Hence, an aircraft in the nonafterburning mode is most susceptible in the band 3.24–4.18  $\mu\text{m}$  from the rear aspect. The aircraft rear fuselage is the main contributor to aircraft IR signature in the forward and side aspects in the band 8.20–11.80  $\mu\text{m}$ , and in

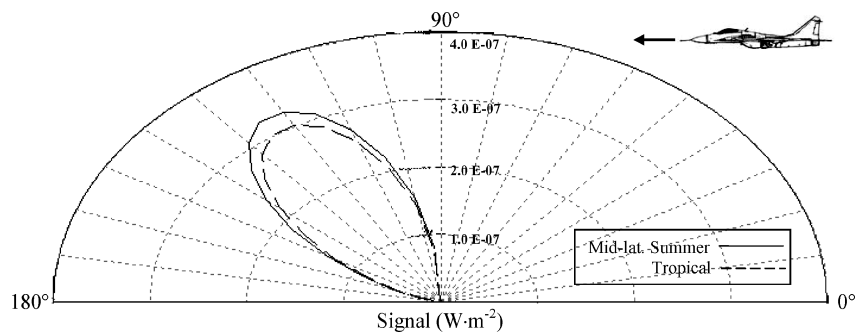


Fig. 15 Irradiance on missile IR seeker in the band 1.95–2.5  $\mu\text{m}$ .

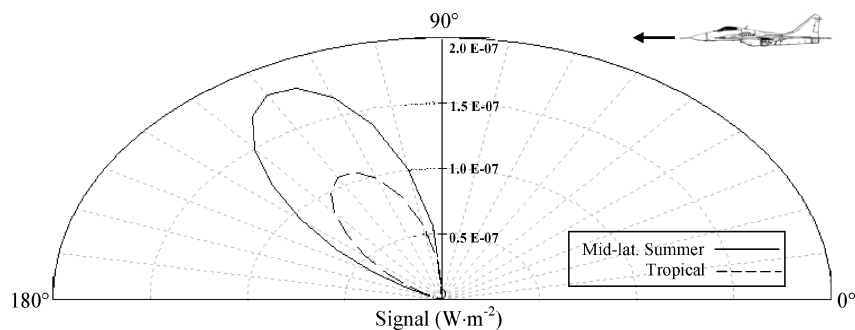


Fig. 16 Irradiance on missile IR seeker in the band 2.92–3.20  $\mu\text{m}$ .

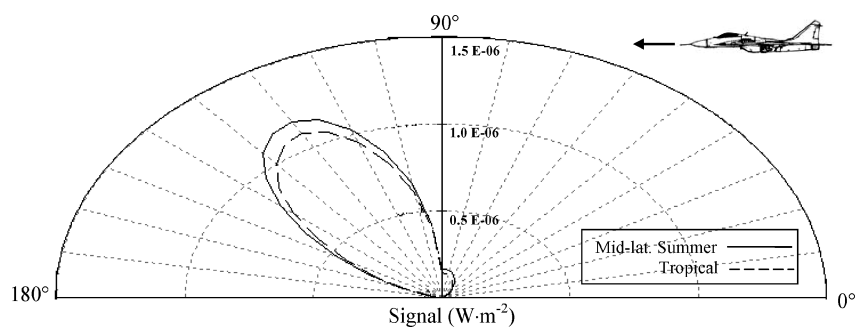


Fig. 17 Irradiance on missile IR seeker in the band 3.24–4.18  $\mu\text{m}$ .

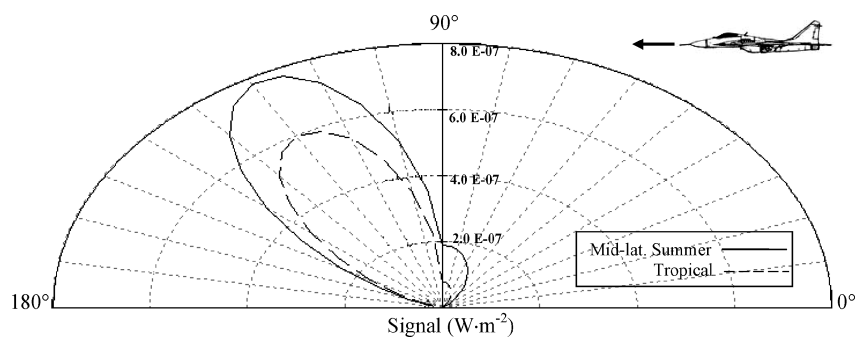


Fig. 18 Irradiance on missile IR seeker in the band 4.50–4.93  $\mu\text{m}$ .

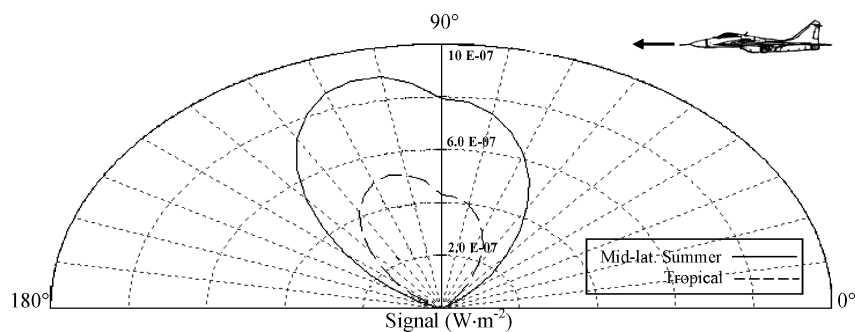


Fig. 19 Irradiance on missile IR seeker in the band 8.20–11.80  $\mu\text{m}$ .

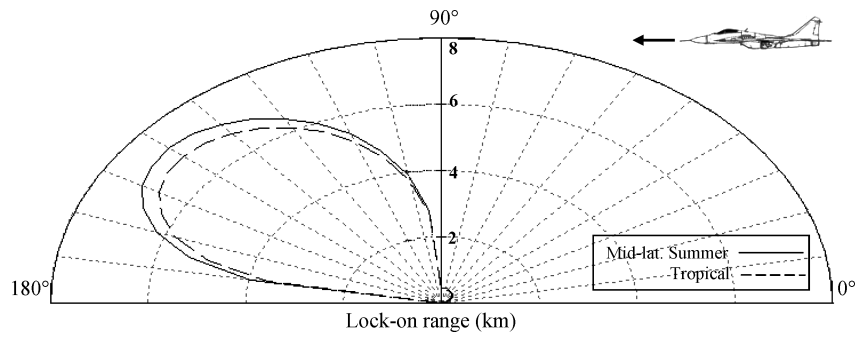


Fig. 20 Variation of aircraft lock-on range in the band 1.95–2.50  $\mu\text{m}$ .

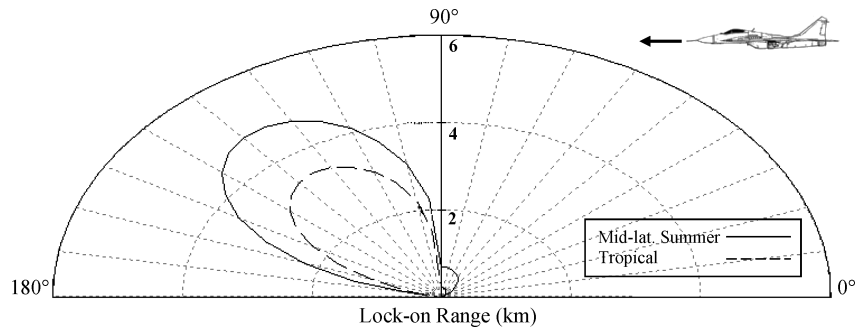


Fig. 21 Variation of aircraft lock-on range in the band 2.92–3.20  $\mu\text{m}$ .

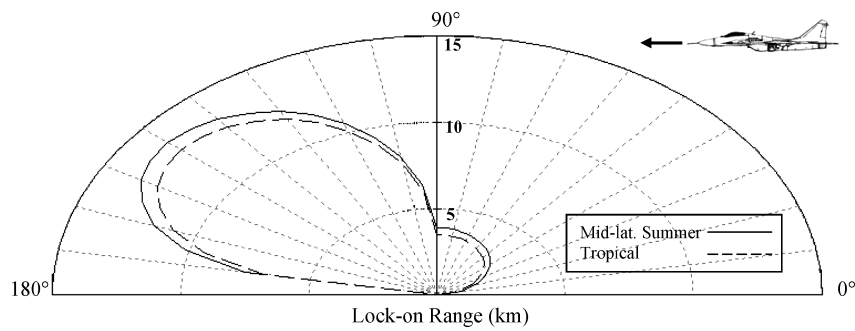


Fig. 22 Variation of aircraft lock-on range in the band 3.24–4.18  $\mu\text{m}$ .

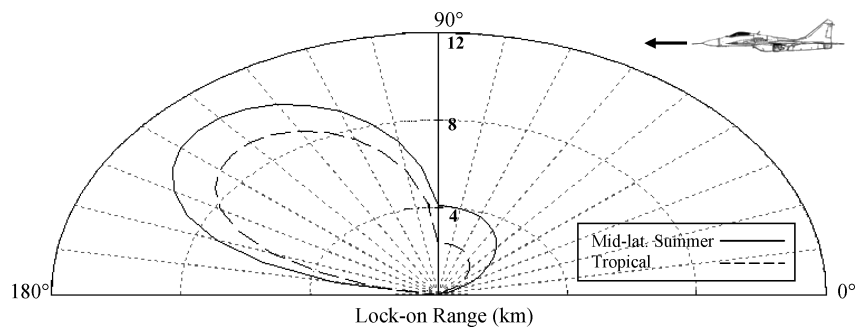


Fig. 23 Variation of aircraft lock-on range in the band 4.50–4.93  $\mu\text{m}$ .

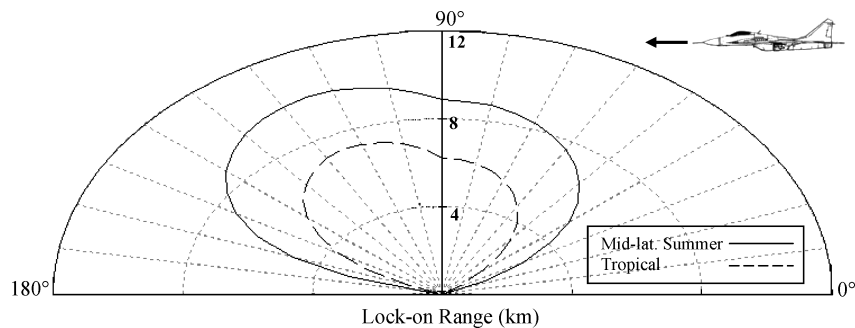


Fig. 24 Variation of aircraft lock-on range in the band 8.20–11.80  $\mu\text{m}$ .



this band the lock-on range in the forward aspect against a typical SAM exceeds 9 km. In the other bands, the lock-on range in the forward aspect is not significant. Consequently, a SAM must operate in the band 8.20–11.80  $\mu\text{m}$  to engage an oncoming aircraft, and in the band 3.24–4.18  $\mu\text{m}$  to engage an aircraft from the rear (revenge shot).

### Conclusions

1) Atmospheric transmittance and radiance have a significant role in dictating infrared signature levels of aircraft, and hence aircraft susceptibility in hostile environments.

2) Atmospheric radiance is dominant only in the band 8–12  $\mu\text{m}$  and does not affect evaluation of aircraft IR signatures in the near and mid IR bands.

3) Assuming atmospheric radiance to be that of a blackbody at ground-level temperature underestimates the computed aircraft IR signature in the band 8–12  $\mu\text{m}$ .

4) The wavelength bands in which the aircraft infrared signature level is significant are 1.95–2.50, 2.92–3.20, 3.24–4.18, 4.50–4.93, and 8.20–11.80  $\mu\text{m}$ .

5) Engine tail pipe contributes more than rear fuselage toward the overall aircraft IR signature level. Hence, aircraft IR signature level is more prominent in the aircraft rear aspect.

6) Aircraft rear fuselage is a prominent source of IR signature level (in the band 8–12  $\mu\text{m}$ ) in the forward and side aspects (during ingress mode). Hence, the aircraft is most susceptible to SAMs in the band 8.20–11.80  $\mu\text{m}$  in the forward aspect.

7) Aircraft IR signature level is at a maximum in the band 3.24–4.18  $\mu\text{m}$  from aircraft rear aspect. Hence, the aircraft is most susceptible to SAMs in the band 3.24–4.18  $\mu\text{m}$  in the rear aspect.

### Acknowledgments

The authors are grateful to the Aeronautics Research and Development Board (Propulsion Panel), Ministry of Defence, Government of India, for the financial support. The authors wish to express their heartfelt gratitude to the reviewers of the *Journal of Aircraft* for the extremely valuable suggestions for modifying the paper. The authors sincerely appreciate the prompt and meticulous processing of this paper by Mr. Kenneth J. Holt, Associate Editor, *Journal of Aircraft*. The authors thank Prof. S.K. Sane and Prof. A.G. Marathe, Dept. of Aerospace Engg. IIT Bombay, for their encouragement and suggestions. The authors thank the A. von Humboldt Foundation, Germany, for the rich exposure to research.

### References

- <sup>1</sup>Rao, G. A., and Mahulikar, S. P., "Integrated Review of Stealth Technology and Its Role in Airpower," *The Aeronautical Journal*, Vol. 106, No. 1066, 2002, pp. 629–641.
- <sup>2</sup>Mahulikar, S. P., Sane, S. K., Gaitonde, U. N., and Marathe, A. G., "Numerical Studies of Infrared Signature Levels of Complete Aircraft," *The*

*Aeronautical Journal*, Vol. 105, No. 1046, 2001, pp. 185–192.

<sup>3</sup>Sully, P. R., VanDam, D., Bird, J., and Luisi, D., "Development of a Tactical Helicopter Infrared Signature Suppression (IRSS) System," AGARD CP-592, 1997.

<sup>4</sup>Sizov, V. V., "Infrared Detectors: Outlook and Means," *Semiconductor Physics, Quantum Electronics and Optoelectronics*, Vol. 3, No. 1, 2000, pp. 52–58.

<sup>5</sup>Bell, W. A., and Glasgow, B. B., "Impact of Advances in Imaging Infrared Detectors on Anti-Aircraft Missile Performance," *Proceedings of SPIE*, Vol. 3701, July 1999, pp. 244–253.

<sup>6</sup>Thompson, J., and Birk, A. M., "Design of Infrared Signature Suppressor for the Bell 205 (UH-1H) Helicopter, I: Aerothermal Design," 46th Annual Canadian Aeronautics and Space Institute (CASI) Conference, May 1999.

<sup>7</sup>Thompson, J., Gubbels, A. W., Barry, B., and Birk, A. M., "Design of an Infrared Signature Suppression for the Bell 205(UH1-H) Helicopter, II: Engine and Flight Testing," 46th Annual Canadian Aeronautics and Space Institute (CASI) Conference, May 1999.

<sup>8</sup>Hudson, D. R., Jr., *Infrared System Engineering*, Wiley, New York, 1969.

<sup>9</sup>Kneizys, F. X., Shettle, E. P., Gallery, W. O., Chetwynd, J. H., Abreu, L. W., Selby, J. E. A., Clough, S. A., and Fenn, R. W., "Atmospheric Transmittance/Radiance: Computer Code LOWTRAN 6," AFGL Report AFGL-TR-83-0187, 1983.

<sup>10</sup>Lowtran 7 Computer Code: User's Manual, AFGL-TR-88-0177, 1988.

<sup>11</sup>Bennet, H. E., Bennet, M. J., and Nagel, R. M., "Distribution of Infrared Radiance Over a Clear Sky," *Journal of the Optical Society of America*, Vol. 50, No. 2, 1960, pp. 100–106.

<sup>12</sup>Bell, E. E., Eisner, L., Young, J., and Oetjen, R. A., "Spectral Radiance of Sky and Terrain at Wavelength Between 1 and 20 Microns. II. Sky Measurements," *Journal of the Optical Society of America*, Vol. 50, No. 12, 1960, pp. 1313–1320.

<sup>13</sup>Berdahl, P., and Fromberg, R., "The Thermal Radiance of Clear Skies," *Solar Energy*, Vol. 29, No. 4, 1982, pp. 299–314.

<sup>14</sup>Mahulikar, S. P., "Prediction of Engine Casing Temperature of Fighter Aircraft for Infrared Signature Studies," *Proceedings of SAE's Aerospace Atlantic Conference*, 1992: SAE Technical Paper 920961, p. 12.

<sup>15</sup>Berdahl, P., and Martin, M., "Emissivity of Clear Skies," *Solar Energy*, Vol. 32, No. 5, 1984, pp. 663–664.

<sup>16</sup>Berger, X., Burriot, D., and Garner, F., "About the Equivalent Radiative Temperatures for Clear Skies," *Solar Energy*, Vol. 32, No. 6, 1984, pp. 725–733.

<sup>17</sup>Berger, X., "A Simple Model for Computing the Spectral Radiance of Clear Skies," *Solar Energy*, Vol. 40, No. 4, 1988, pp. 321–333.

<sup>18</sup>Berger, X., and Bathiebo, J., "From Spectral Clear Sky Emissivity to Total Clear Sky Emissivity," *Solar and Wind Technology*, Vol. 6, No. 5, 1989, pp. 551–556.

<sup>19</sup>Berger, X., and Bathiebo, J., "Directional Spectral Emissivities of Clear Sky," *Renewable Energy*, Vol. 28, No. 12, 2003, pp. 1925–1933.

<sup>20</sup>Mahulikar, S. P., Kolhe, P. S., and Rao, G. A., "Skin Temperature Prediction of Aircraft Rear Fuselage with Multi-Mode Thermal Model," *Journal of Thermophysics and Heat Transfer*, Vol. 19, No. 1, 2005, pp. 114–124.

<sup>21</sup>Eisner, L., Bell, E. E., Young, J., and Oetjen, R. A., "Spectral Radiance of Sky and Terrain at Wavelengths Between 1 and 20  $\mu$ , III: Terrain Measurements," *Journal of Optical Society of America*, Vol. 52, No. 2, 1962, pp. 201–209.